Technical University of Denmark

DTU

Application of the fluid dynamics model to the field of fibre reinforced self-compacting concrete

Svec, Oldrich; Skocek, Jan; Stang, Henrik; Olesen, John Forbes; Thrane, L.N.

[Link back to DTU Orbit](#)

DTU Library
Technical Information Center of Denmark

Application of the fluid dynamics model to the field of fibre reinforced self-compacting concrete

O. Svec[1], J. Skocek[1], H. Stang[1], J. F. Olesen[1], L. N. Thrane[2]

[1] *Technical University of Denmark, Department of Civil Engineering, {olsv, hs, jfo}@byg.dtu.dk*
[2] *Danish Technological Institute, lnth@teknologisk.dk*

1   Abstract

Ability to properly simulate a form filling process with steel fibre reinforced self-compacting concrete is a challenging task. Such simulations may clarify the evolution of fibre orientation and distribution which in turn significantly influences final mechanical properties of the cast body. We have developed such a computational model and briefly introduce it in this paper. The main focus of the paper is towards validation of the ability of the model to properly mimic the flow of the fibre reinforced self-compacting concrete. An experiment was conducted where a square slab was filled with the fibre reinforced self-compacting concrete. A computational tomography scanner together with an image analysis were used to obtain a field of fibre orientation tensors. These tensors were compared to the tensors obtained by the simulation. The comparison shows the ability of the model to predict the real behaviour of the self-compacting fibre reinforced concrete.

2   Introduction

Concrete is a complex material. Its composition makes it extremely difficult to predict the final detailed behaviour of structural elements. Adding steel fibres to self-compacting concrete makes the concrete even more unpredictable. It cannot be assumed to be an isotropic material any more since the fibres orient and disperse during the flow. The knowledge of the final orientation and dispersion of fibres in the structural elements could provide a basis for understanding how the fibres influence the final mechanical properties of the structural elements.

Experimental work leading to the knowledge of orientation and dispersion of fibres is often a very time and resource consuming procedure. One has to do the casting of the elements. The cast element has to be left to harden, cut into pieces and only then a computational tomography (CT) scanner can be used to obtain the 3D image of the fibres in the elements. However, only small parts of the elements can be CT scanned due to the fast overheating of the device. Another option could be to cut the element into many slices and then visually compute the number and position of individual fibres along these sections [1]. A completely different approach might be to use a transparent yield stress fluid such as Carbopol [2] to replace the fluid matrix of self-compacting concrete. All these approaches are not simple and, therefore, only a limited amount of information is obtained from such experiments. On the other hand, numerical simulations are limited only by the computational power. A simulation tool capable of simulating a flow of self-compacting concrete together with fibres and the largest aggregates could provide a sufficient alternative for obtaining the required information.

In this paper, we introduce such a model. We further present a comparison of the simulation model with a real-world experiment. At the end of the paper, we show that our model predicts the final orienta-

tion of fibres sufficiently well and in a reasonable amount of time.

3   Methods

In this section, we present the two-way coupled model for the flow of suspensions of rigid solid particles in a non-Newtonian fluid. The model consists of the fluid dynamics part used to predict the free surface flow of a homogeneous fluid. The model is also capable of predicting the time and space evolution of the solid particle suspensions.

Due to the diversity of the individual phenomena, the overall model is separated into three distinct levels (Figure 1):

a) **Level of fluid:** Flow of a non-Newtonian free surface fluid is solved at this level. The Lattice Boltzmann method [3, 4] is used as the fluid dynamics solver whereas the Mass Tracking Algorithm describes the free surface of the flow. This level is influenced by the interaction forces coming from the "Level of fluid - solid particles interaction".

b) **Level of fluid - solid particles interaction:** This intermediate level provides a communication channel between the "Level of fluid" and the "Level of solid particles". The communication takes place via force interactions. We have used the Immersed boundary method with direct forcing [5] to accommodate the communication between the two levels. No-slip boundary condition between the fluid and the solid particles is enforced. To satisfy this condition, an interaction force is created and sent back to the "Level of fluid" and the "Level of solid particles".

c) **Level of solid particles:** Solid particles with an exact analytical geometry are used at this level. The dynamics of the solid particles is solved using Newton's equations of motion. Interactions among the solid particles and between the solid particles and the boundaries (such as walls etc.) are also solved. This level is influenced by the interaction forces coming from the "Level of fluid - solid particles interaction".
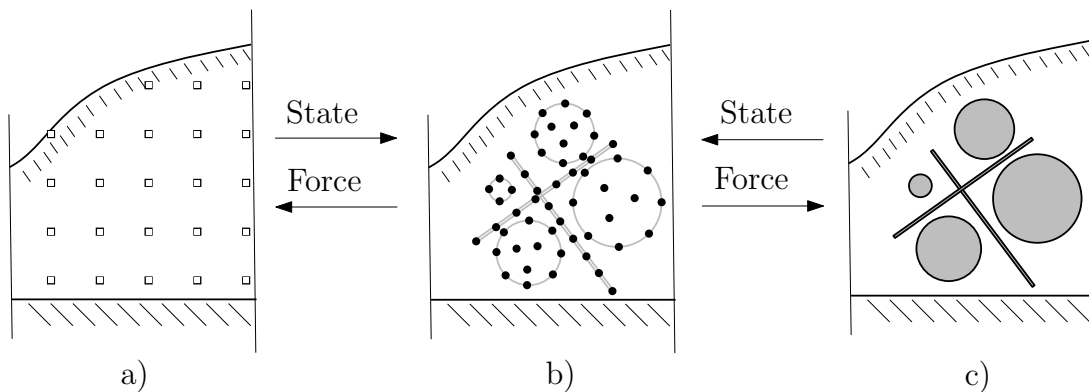

Figure 1: Scheme of the model. a) Level of fluid, b) Level of fluid - solid particles interaction, c) Level of solid particles.

3.1   Level of fluid

Level of fluid solves the flow of a homogeneous non-Newtonian free surface fluid and thus consists of the fluid dynamics and free surface solver.

2

3.1.1 Fluid dynamics solver

In contrast to the traditional computational fluid dynamics methods, where the problem is formulated by means of macroscopic quantities such as space and time dependent velocity and pressure fields, the Lattice Boltzmann method, with its roots in the kinetic theory of gases, treats the fluid as clouds of microscopic particles (e.g. molecules). Individual microscopic particles are assumed to be freely propagating through the space while instantaneously colliding among each other from time to time (see Lattice gas cellular automata [3]). The clouds of particles are approximated by continuous particle distribution functions (i.e. probability of a particle occurrence). The particle distribution functions are further discretized by a set of discrete particle distributions to limit the number of unknowns. Lattice Boltzmann equation provides rules for mutual collisions and propagation of the particle distributions. The macroscopic quantities (density, velocity et.) can then be computed as moments of the particle distributions.

The computational domain is typically discretized by a set of Eulerian cells[1] of a uniform size (see Figure 1a). Continuous fields of macroscopic quantities (such as velocity fields) are then approximated by the mean values of the quantities in the discretized cells. Similarly, the time is discretized into uniform time steps.

In a given time step, the state of the fluid in a cell is fully described by the particle distributions in that cell. The particle distributions in the given time step at a certain position are computed from the particle distributions in neighbouring cells in the previous step. This accounts for the propagation of the particle distributions. Collisions of the particle distributions are in the simplest case approximated by a linear transformation of the particle distributions towards the local equilibrium state. Such a transformation is called Bhatnagar-Gross-Krook collision operator [6]. The local equilibrium state is based on the Maxwell-Boltzmann distribution, and is computed from the local macroscopic velocity and pressure (density) of the fluid.

3.1.2 Free surface algorithm

A free surface has been implemented in the form of the Mass Tracking Algorithm [7]. The algorithm makes use of the same Eulerian discretized domain as the Lattice Boltzmann method where fluid, gas and interface cells are introduced. The Lattice Boltzmann equation is computed in the fluid and interface cells, only. Gas cells are empty cells where nothing is computed. Interface cells separate fluid phase and gas phase and are therefore responsible for a correct implementation of the free surface algorithm and for the correct mass conservation of the fluid. Interface cells are moreover the only place where the Mass Tracking Algorithm comes into play in the form of local mass tracking and reconstruction of missing information from the gas phase.

3.2 Level of fluid - solid particles interaction

The Immersed boundary method with direct forcing [5] provides a direct linkage between the "Level of fluid" and the "Level of solid particles". The fluid can "feel" the solid particles in the form of a force field. In the same manner, the solid particles can "feel" the fluid in the form of forces acting on the solid particles. At this level, the solid particles are discretized into a set of Lagrangian nodes[2] (see black circle marks in Figure 1b). It is assumed that the velocity of a solid particle and the fluid at the same Lagrangian node are equal due to the no-slip boundary condition. Non-equal velocities are transformed into a force field acting on both the particle and the fluid. The force is in the simplest form computed based on Newton's second law of motion (i.e. such a force to accelerate a certain volume of the fluid

---

[1]Nodes fixed in space

[2]Position of the nodes evolves in time

that is surrounding the Lagrangian node to the velocity of the solid particle at that Lagrangian node). Since the Lagrangian nodes usually do not coincide with the Eulerian nodes (coming from the "Level of fluid"), the velocity of the fluid in the Lagrangian nodes is obtained by a volume averaging of the velocities at the Eulerian nodes. The volume averaging is conducted by means of a Dirac delta function [8]. The resulting forces are usually extrapolated from the Lagrangian nodes back to the Eulerian nodes (i.e. to the "Level of fluid") using the same Dirac delta function.

The Immersed Boundary Method provides, contrary to other methods (e.g. bounce-back wall scheme [9, 10]), smooth and stable time evolution of all the quantities (i.e. the position of the solid particles or forces acting on them). The most important feature of the Immersed Boundary Method, however, is its ability to simulate small objects of only a few lattice units or even sub-grid sized objects, see [11]. This results in a significant reduction of the computational time needed.

3.3 Level of solid particles

At this level, the solid particles are assumed to be rigid bodies of a simple geometric shape (sphere, ellipsoid or cylinder) with the ability to move, rotate and interact among each other, with fluid, walls and other obstacles. The dynamics of those immersed solid particles is driven by Newton's second law of motion which is discretized with the explicit Runge-Kutta-Fehlberg time integration scheme with an adaptive time step. The numerical integration scheme that we adopted ensures the stability and accuracy of the simulation even for a highly non-linear behaviour.

An accurate and robust treatment of interactions among the solid particles and between the solid particles and other obstacles such as walls or reinforcement plays an important role in a proper description of the relevant phenomena. The model includes two types of interactions, namely mutual instantaneous collisions of solid particles and continuous forcing of a general type. The instantaneous collisions were approximated by means of force impulses [12]. An example of the continuous forcing could be a lubrication force correcting the fluid flow between two solid particles in the case when the two solid particles approach each other to a sub-grid distance [13].

4 Applications

Any simulation tool should be validated preferably against both analytical solutions and as many experiments as possible. The in-depth description of the presented model and its basic validation was performed in [12]. The main task of this paper is to show the capability of the model to properly describe the complex behaviour of fibre suspension in a self-compacting concrete. To do so, the orientation of fibres as a result of the simulation model is compared with the orientation of fibres in the real experiment.

4.1 Plate experiment

The plate experiment was conducted by the Danish Technological Institute where a plate of size 1.6 x 1.6 x 0.15 m was cast (see Figure 2a). The casting was performed from a circular inlet with a diameter of 20 cm and positioned in the corner of the plate at a distance of 300 mm from the sides of the slab. The speed of filling was 2 m/s. Density of the self-compacting concrete was approximately 2300 kg/m^3 whereas density of the fibres was 7850 kg/m^3. Bingham rheology parameters, i.e. plastic viscosity and yield stress, of the suspension of steel fibres in the self-compacting concrete were measured using 4C-Rheometer [14]. The averaged resulting values at the time of casting were 45 Pa and 75 Pa s for the yield stress and the plastic viscosity, respectively. A volume fraction of 0.5 % of straight steel fibres with
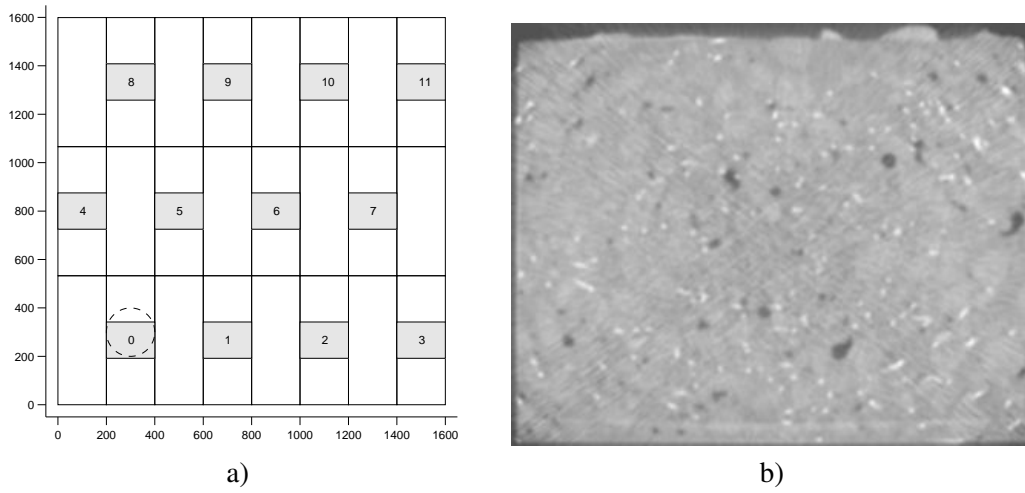
Figure 2: a) Scheme of the plate. White rectangles represent the standard beams. Grey rectangles stand for the CT scanned regions. The dashed circle mark is the inlet. b) An example of a CT scanned slice. White regions represent sections of the steel fibres whereas dark regions are the air voids.

hooked ends (Bekaert Dramix RL 80/60 BN) were used in the experiment, corresponding to 40 kg/m^3.

The casting lasted for approximately 30 seconds. The plate was left to harden for 28 days and then cut into 24 standard sized beams. "HiSpeed CT/i" scanner produced by "Ge Medical Systems" was used to scan 12 middle sections of the chosen standard beams (see grey rectangles in Figure 2a). The dimensions of the scanned volume were 200 x 150 x 150 mm. A set of DICOM images was obtained as the output of the CT scanner where each image represented a slice of the specimen (see Figure 2b). A 3D model was reconstructed from the series of slices (see Figure 3a). A 3D thresholding technique was used to remove the concrete and the air voids (i.e. the dark regions). Subsequently, a 3D skeletonization technique was applied to obtain a set of 3D lines (see Figure 3b).

The orientation of fibres in individual regions was represented by means of second order orientation tensors similarly to [15]. The orientation tensors were visualized in the form 3D ellipsoids and in this paper in the form of 2D ellipses (see Figure 4). The orientation of the ellipses represent the mean orientation of fibres in the region. Aspect ratio of the ellipses represents the alignment of fibres in the region. High aspect ratio of the ellipses corresponds to a high alignment of the fibres and vice versa the circular shape of the ellipses corresponds to a uniformly random orientation of fibres.
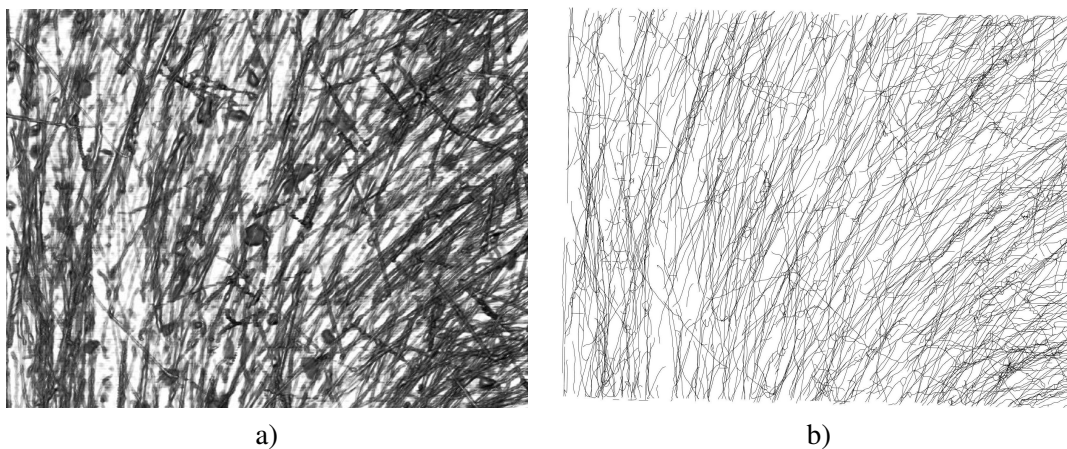

Figure 3: a) Top view of the 3D model. b) Top view of the thresholded and skeletonized 3D model of the CT scanned sample.

The main outcome of the experiment was a set of 3D ellipsoids representing the orientation of fibres in the plate. Figure 4 presents two top views of the plate together with orientation ellipses in the CT scanned regions. The upper third and the lower third of the plate are shown in the figure to highlight the differences in ellipses through the depth of the plate.

One may notice that the fibres orient quite significantly. The fibres tend to orient normal to the flow direction which forms a circular pattern. The longer the distance from the inlet the more the orientation of fibres increase. The fibres in the bottom third of the plate seem to be more randomly distributed in comparison to the upper third of the plate but the difference is not that pronounced.

This was surprising, as the presented simulation predicted an almost complete randomness of the fibre orientation in the bottom third of the plate. A reasonable explanation might be a boundary effect as described in [16]. An apparent Navier's slip [17] probably occurred during the experiment and should be taken into account in the simulation.

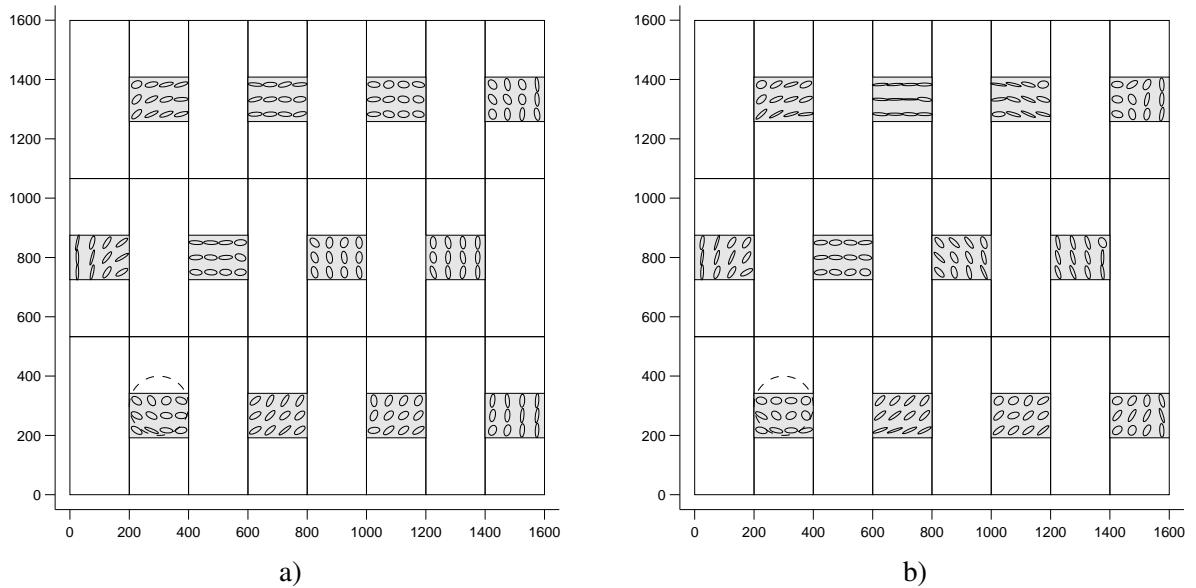a)   b)

Figure 4: Top view of the lower (a) and upper (b) third of the plate cut into standard beams (white rectangles). Ellipses represent fibre orientations of the CT scanned regions (grey rectangles).

4.2 Plate simulation

A simulation of the aforementioned plate was run using the model introduced in the Section 3 (see Figure 5). All the parameters (geometry, rheology) were taken from the experiment. Coulomb friction was applied among the fibres and between the fibres and the boundary condition. The values of static and dynamic friction were both set to 0.3. In addition, all the collisions of the fibres were assumed to be plastic, i.e. coefficient of restitution was set to 0.

The computational domain of the fluid was discretized by 1 cm = 1 lattice units. Length and diameter of the discretized fibres was then 6 and 0.075 lattice units. A correction term of the forcing evaluated by the Immersed boundary method (introduced in [11]), which allows for sub-grid sized diameters of the fibres, was applied during the simulation. The overall domain was spatially parallelized, i.e. sub-divided into 25 sub-domains (see Figure 5 right) to speed up the computations. The computation started with one running sub-domain, adding additional sub-domains as the flow spread. The total number of fibres reached 72 433, i.e. ca. 2900 fibres per sub-domain. The simulation was run on 32 cores Intel Xeon X7550 2.00 GHz with 64 GB RAM and took approx. 1 week of computations. Approximately 95 % of the computational power was spent on solving the "Level of solid particles" and the "Level of fluid
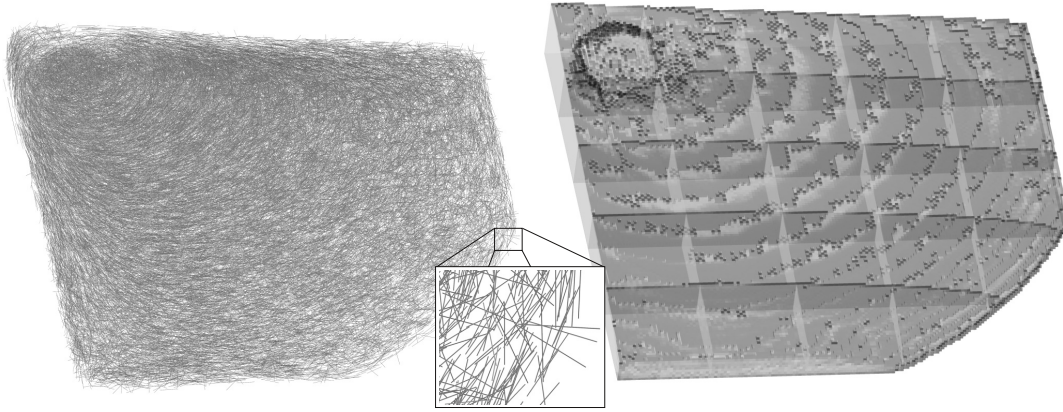
Figure 5: A 3D view of the fibres (left) and the fluid (right) during the simulation.
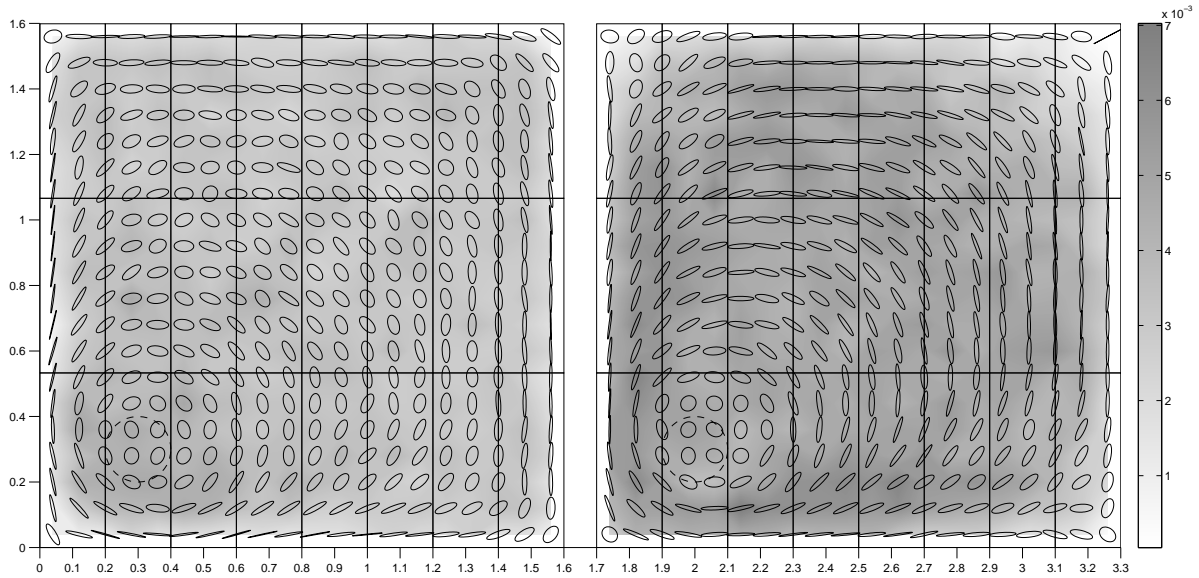

Figure 6: Top view of the lower (left) and upper (right) third of the plate at the end of the simulation. The grey scale stands for an estimate of the fibre volume fraction.

- solid particles interaction". Only 5 % of the computation power was spent on solving the "Level of fluid". The final orientation of fibres obtained from the simulation is presented in Figure 6.

As mentioned in the previous section, an apparent slip occurred during the experiment. There are at least two ways to incorporate the apparent slip into the simulation model. The most obvious one is to include a thin layer of a fluid with reduced viscosity near the form-work. This approach creates troubles with the stability of the model due to high differences in the viscosities in the domain. A numerical time step would have to be significantly reduced leading to a high increase of the computational time. We have therefore decided to use a more "artifical" way of describing the apparent slip, i.e. the "molecular slip" as described in [18]. The advantage of such an approach is the stability of the model even for high values of the apparent slip. The disadvantage is that there is no direct relation between the real apparent slip and the "molecular slip" and, therefore, the value has to be fitted. We ran the simulation with a slip coefficient of 0.85, 0.9, 0.95 and 1.0, and observed the best correlation with the experiment with the values of 0.9 and 0.95. Figure 6 presents the results where a slip coefficient of 0.9 was used.

5 Comparison

Figure 7 presents a comparison of the orientation ellipses obtained from the simulation (solid red) with the orientation ellipses obtained from the experiment (dashed black) in the CT scanned regions. There seems to be a nice correlation between the experiment and the simulation in most places. Near to the inlet, the ellipses do not match perfectly which is probably caused by a slightly inaccurate positioning of the inlet in the simulation as compared to the experiment.
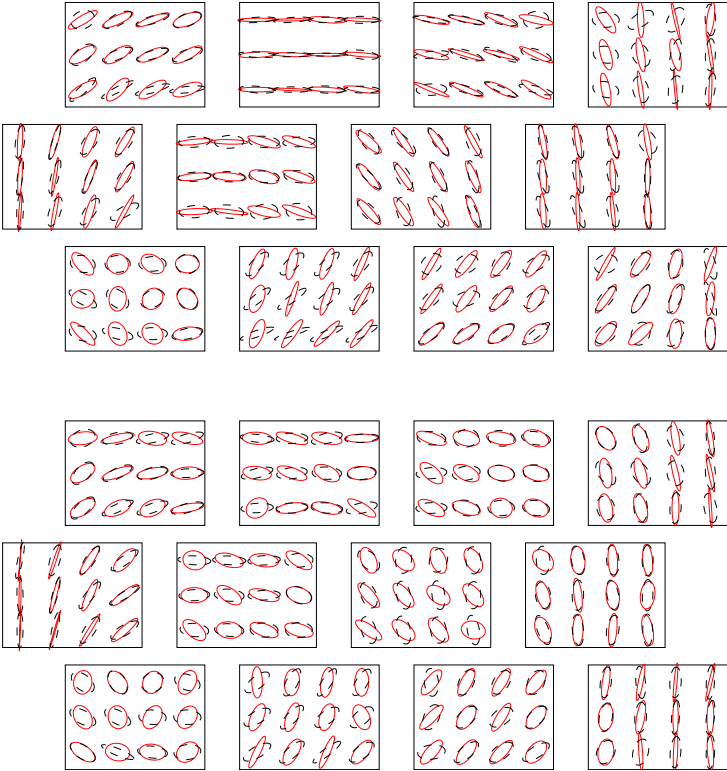

Figure 7: Comparison of the CT scanned ellipses (dashed black) and ellipses obtained by the simulation (solid red). Top part shows the upper third of the plate whereas the bottom part present the lower third of the plate.

6 Conclusions

A model capable of simulating the flow of fibre reinforced self-compacting concrete was presented. An experiment was conducted to show the abilities of the model to correctly describe the final orientation of fibres. A plate was filled with the fibre reinforced self-compacting concrete, left to harden, cut into standard sized beams and scanned by a CT scanner. Ellipses were then constructed to represent the fibre orientation in different regions. A simulation was run with the experimentally established parameters and the orientation ellipses were compared to the experiment.

The comparison showed capability of the model to simulate the flow of fibre reinforced self-compacting concrete with a sufficient accuracy and in a reasonable amount of time. It was also pointed out, how crucial a correct value of the apparent slip is, to obtain the correct orientation of fibres.

7 Acknowledgements

References

[1] Elena Vidal Sarmiento. *Influence of concrete flow on the mechanical properties of ordinary and fibre reinforced concrete*. PhD thesis, Technical University of Catalonia, 2011.

[2] Oldrich Svec, Jan Skocek, John Forbes Olesen, and Henrik Stang. Fibre reinforced self-compacting concrete flow simulations in comparison with L-Box experiments using Carbopol. In *Proceedings of BEFIB*, 2012.

[3] Dieter A. Wolf-Gladrow. *Lattice-Gas Cellular Automata and Lattice Boltzmann Models: An Introduction (Lecture Notes in Mathematics)*. Springer, 2000.

[4] Michael C. Sukop and Daniel T. Thorne. *Lattice Boltzmann Modeling: An Introduction for Geoscientists and Engineers*. Springer, 2005.

[5] Z Feng and E Michaelides. Proteus: a direct forcing method in the simulations of particulate flows. *Journal of Computational Physics*, 202(1):20–51, January 2005.

[6] Shiyi Chen and Gary D. Doolen. Lattice Boltzmann method for fluid flows. *Annual Review of Fluid Mechanics*, 30(1):329–364, January 1998.

[7] C. Körner, M. Thies, T. Hofmann, N. Thürey, and U. Rüde. Lattice Boltzmann Model for Free Surface Flow for Modeling Foaming. *Journal of Statistical Physics*, 121(1-2):179–196, October 2005.

[8] Xiaolei Yang, Xing Zhang, Zhilin Li, and Guo-Wei He. A smoothing technique for discrete delta functions with application to immersed boundary method in moving boundary simulations. *Journal of Computational Physics*, 228(20):7821–7836, November 2009.

[9] AJC Ladd. Numerical simulations of particulate suspensions via a discretized Boltzmann equation. Part 1. Theoretical foundation. *Journal of Fluid Mechanics*, 211, 1994.

[10] A.J.C. Ladd. Numerical simulations of particulate suspensions via a discretized Boltzmann equation. Part 2. Numerical results. *Journal of Fluid Mechanics*, 271(1):311–339, 1994.

[11] Oldrich Svec, Jan Skocek, Henrik Stang, John Forbes Olesen, and Peter Noe Poulsen. Flow simulation of fiber reinforced self compacting concrete using Lattice Boltzmann method. In *Proceedings of ICCC*, 2011.

[12] Oldrich Svec and Jan Skocek. Model predicting the flow of a suspension of rigid solid particles in a non-Newtonian fluid. *To be published*, 2012.

[13] N.-Q. Nguyen and A. Ladd. Lubrication corrections for lattice-Boltzmann simulations of particle suspensions. *Physical Review E*, 66(4):1–12, October 2002.

[14] Lars Nyholm Thrane, Pede Claus, and Claus V. Nielsen. Determination of Rheology of Self-Consolidating Concrete Using the 4C-Rheometer and How to Make Use of the Results. *Journal of ASTM International*, 2009.

[15] Suresh G. Advani. The Use of Tensors to Describe and Predict Fiber Orientation in Short Fiber Composites. *Journal of Rheology*, 31(8):751, 1987.

[16] Stefan Jacobsen, Hedda Vikan, and Lars Haugan. Flow of SCC along Surfaces. In Kamal Henri Khayat and Dimitri Feys, editors, *Design, Production and Placement of Self-Consolidating Concrete*, pages 163–173. Springer Netherlands, 2010.

[17] Lars Nyholm Thrane. *Form Filling with Self-Compacting Concrete*. PhD thesis, Technical University of Denmark, 2007.

[18] P LAVALLEE, J BOON, and A NOULLEZ. Boundaries in lattice gas flows. *Physica D: Nonlinear Phenomena*, 47(1-2):233–240, January 1991.